Journal of Manufacturing Systems
Vol. 23/No. 4
2004

Automated Torch Path Planning Using Polygon Subdivision for Solid Freeform Fabrication Based on Welding

Rajeev Dwivedi and **Radovan Kovacevic,** Research Center for Advanced Manufacturing, Southern Methodist University, Dallas, Texas, USA

Abstract

A continuous path is one of the most important requirements for solid freeform fabrication (SFF) based on welding. This paper proposes a method for torch path planning applicable to SFF based on welding with an emphasis on minimum human intervention. The suggested approach describes a method based on the subdivision of a two-dimensional (2-D) polygonal section into a set of monotone polygons to generate a continuous path for material deposition. A two-dimensional contour is subdivided into smaller polygons (subpolygons). The path for each individual subpolygon is generated. The final torch path is obtained by connecting individual paths for all the subpolygons and trimming along the points of intersection of the paths for individual subpolygons. The final path is a closed loop; therefore, any point can be selected as the starting point for material deposition. The proposed method can be used to develop the toolpath for CNC milling.

Keywords: *Solid Freeform Fabrication, Monotone Chain, Zig-Zag Path, Upturn Vertex, Downturn Vertex, Subpolygon*

Introduction

Solid freeform fabrication (SFF) was envisioned as the creation of three-dimensional objects directly from the CAD files without human intervention. It was intended for the conceptualization of a design. Today, SFF is used not only for obtaining the physical prototypes but for building functional parts as well. SFF based on deposition by welding is intended to manufacture the functional parts.

Common to all SFF techniques is the basic approach. First, the physical part to be built is modeled in the CAD system (*Figure 1*). The next process involves slicing the three-dimensional solid model of the object by a set of parallel planes. The intersection of the parallel planes with the external surface of the object provides a set of contours. At the end, process parameters are set, and the torch path is generated to deposit material in the interior of each contour to generate a layer. The process of filling in the interior of the layer is accomplished by path planning. Contrary to most existing path planning techniques, which are based on the toggle in the state of the energy medium such as the laser, the requirements for path planning for SFF based on welding are unique. The inherent properties of the welding-based deposition require that the path must be continuous over the cross-sectional area of deposition.

Of the other path planning approaches used in SFF, the raster scanning pattern technique (Crawford, Das, and Beaman 1991; Rock and Wozny 1991) is based on the planar ray casting along one direction and toggling over the geometry of the cross section. However, this path planning approach is not applicable to welding-based rapid prototyping due to the frequent variation in electric arc status. Another approach to path planning is based on a variety of replicating hatch-and-weave patterns (Jacobs 1992; Ullet et al. 1994; Jayanthi, Keefe, and Gargiulo 1994)—fractal and space curves (Bertoldi et al. 1998). While the patterns have proven to be very effective solutions for various SFF techniques, the limitation of frequent crossover of the path segments and the closely spaced segments lead to accumulation of heat and deformation of the substrate. Offsetting a parametric curve for scan path generation (Venkataramani, Das, and Beaman 1998; Ganesan and Fadel 1994) and parametric contour scanning (Beaman 1992; Chen, Crawford, and Beaman 1996) are based on the generation of the path patterns using C^1 continuity curves, however, the overall path is based on a set of contours that is not connected. The studies and the method suggested by Rajan, Srinivasan, and

This paper is an expanded version of a paper originally presented at NAMRC 31 and published in the *Transactions of NAMRI/SME*, Vol. 31, 2003.

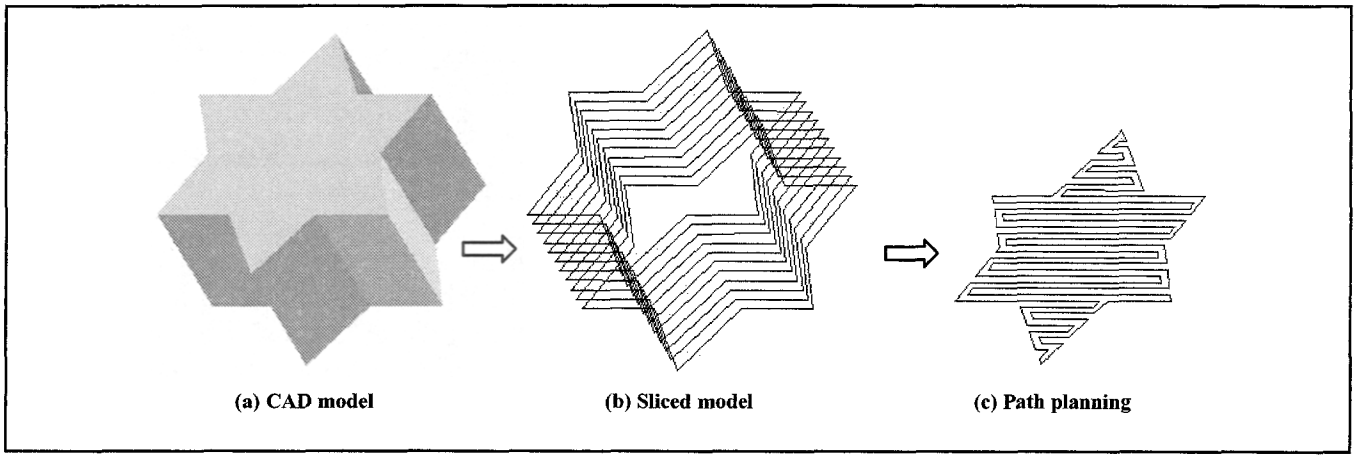

Figure 1
Process Planning for Solid Freefrom Fabrication

Tarabanis (2001) suggest an approach to determine a suitable direction of the path generation for filling a region based on scanning lines of finite width, however, the method does not ensure the connectivity of the path segments. Path planning suggested by Tarabanis (2001) refers to the goal of reducing the amount of supports needed to build the physical prototype of the part by taking advantage of the two novel manufacturing techniques of shelving and bridging that had been developed previously; however, the goal of this approach and the process in which it is applied are different from the requirements and the goal of path planning for rapid prototyping based on welding. Chen et al. (2004) describe a general framework for automated path planning for nanomanufacturing. Collision-free paths are generated for fabrication at the nano scale. The geometry of the cross-sectional area, and hence the toolpath, is trivial and expressed by straight lines that are arranged in a suitable order. The main emphasis is on accessing a given point rather than filling an area. In another work reported by Chen, Xi, and Chen (2004), a material distribution model is developed based on the comparison of continuous material deposition processes for two deposition patterns, raster and spiral. The main emphasis is on the comparison of the two methods, and an approach for a general cross-sectional area is not described. Sheng et al. (2003) suggest a decomposition-based approach for the path planning. Any given region is decomposed into a set of subregions, and the toolpath for each is generated; however, a connectivity among the toolpaths for the subregions is not possible for all the cases.

Toolpath planning for the process of area milling and SFF involves sweeping an area with a tool head, and each sweep of the tool accompanies machining/deposition of a fixed width of material, the path planning for the two processes, are similar. Sufficient literature on the path planning for area milling is available (Sarma 2000; Park and Choi 2000; Li, Dong, and Vickers 1994; Held 1991; Griffiths 1994; Cox et al. 1994). This paper investigates some of the approaches used in area milling toward the development of an algorithm for SFF based on welding. Due to the inherent properties of the two processes, there are several limitations of applying path generation algorithms intended for milling in solid freeform fabrication. Area milling allows a dry run over the region that has already been swept; in SFF, sweeping the same area again will lead to overdeposition of material. In area milling, the height of the tool can be changed when it retraces a region to avoid any tool marks (Park and Choi 2000); however, the same approach for welding-based material deposition requires incorporation of an extra set of parameters for process control and may affect surface quality.

Three common strategies for traversing areas include evolving curves, using spiral curves, and using space-filled curves (Sarma 2000). Of the various schemes used for trajectory planning for shape-creation operations, offsetting and zig-zag curves are the most popular (Sarma 2000). Advantages of offsetting include a smooth finish, less time and material requirements, and better suitability for thin sections. The advantages of the zig-zag scheme include simpler calculations and bypassing the over/underfill problem (Farouki et al. 1994, 1995). In the offsetting scheme, numerous disconnected

closed curves are formed; therefore, it is not suitable for SFF based on welding. Li, Dong, and Vickers (1994) suggested various toolpath patterns for cutting layers with a single island. Their suggestions included component offset, stock/component parallel offset, proportional blending, and max-min offset patterns. However, none of these methods gives a continuous path without sweeping a region that is already swept. Griffiths (1994) reported an algorithm based on Hilbert's curve for a milling machine. The calculated paths maintain continuity between the neighboring areas, but the path is highly convoluted to take into account the machining of a three-dimensional surface. A highly convoluted path may accumulate tremendous heat in the process of SFF based on welding and hence may lead to deformation of the part. A method suggested by Yang et al. (2002) is based on a fractal scanning path for laser sintering. This technique allows space filling, self-avoiding, and self-similar scanning. The method also includes the trimming of fractal curves for arbitrary boundaries by means of judging the intersection between arbitrary boundaries and fractal curves. The geometry of the path causes an accumulation of heat in welding-based solid freeform fabrication and possible deformation of the component. Anand and Egbelu (1994) described a method to generate a zig-zag path for spray painting by creating several parallel lines equidistant to the y-axis. The vertical lines are intersected with appropriate edges of the polygon to define the turning points of the path along the edge of the polygon. The method generates a continuous path for simple polygons, but the retracing of points and inability to generate a continuous path for complex polygons is inherent in it. The method suggested by Park and Choi (2000) calculates a continuous toolpath for direction-parallel area milling. The method involves three modules: (1) finding an optimal inclination, (2) calculating and storing toolpath elements, and (3) toolpath linking. In various cases, however, the path connecting two regions sweeps across the area that is already swept; hence, the method is unsuitable for use in the process for material deposition by welding. This approach, though, provides a better understanding of the effect of orientation.

Cain (1992) reported a technique applicable to image representation. The technique is used for decomposing any arbitrary polygon into trapezoid slabs about the y-coordinate of every vertex to define the slabs. Each trapezoid slab is scan-converted by rasterization circuitry. Fossum (1994) reported another technique applicable to image representation. He suggested to bound a polygon by a rectangle, then subdivide the rectangle into a group of slabs such that each rectangular slab is bounded by a pair of interior vertices of the complex polygon. For each slab, the crossing point of the edges, if any, is determined, and the slab is divided to a sub-slab about the point of crossing. The edges contained within the rectangular slabs are viewed as simple polygons, or trapezoids, which can be filled for display. Simplification of a complex polygon to trapezoids eliminates the complexities, hence, the method can be used to fill material in a cross section for SFF. One drawback of these techniques is that the number of polygons to be filled increases. However, the number of polygons to be filled can be reduced by merging some of the trapezoidal polygons.

This paper introduces a technique of path generation applicable to solid freeform fabrication based on welding. Certain geometric principles used for path generation and the properties of a welding bead are discussed first. Further, a step-by-step approach to generate the path to achieve uniform deposition is discussed in detail.

Path Planning for SFF Based on Deposition by Welding

Mandatory to the CAD representation scheme is the requirement for the closed-surface representation, which defines an enclosed volume $X \in R^3$. The data must specify the inside $p \in X$, outside $p \notin X$ as the complement, and boundary, $p \in \partial X \subset X$, i.e., the subset of solid where any neighborhood contains nonmembers, of the model. This requirement ensures that all the horizontal cross sections of the model are closed curves, which is necessary to create a solid model.

Solid freeform fabrication of a solid functional part, X, by welding involves material deposition to generate the prototype, X', followed by removal of the extra stock of material, $S = X' - X$, to get the desired shape. Process planning transforms the solid model representation of the object to its equivalent process field. The process field is the vector field associated with solid X, $F : R^3 \rightarrow R^m$, that maps a point in Euclidean space to the m-dimensional process space. The m is the total number of process parameter variables. Practically, for a gas tungsten arc welding based solid freeform fabrication, this set

includes the coordinates of the torch path, torch translational speed, torch rotational speed, current input, heat sink, and wire feeding rate. The path is a trajectory followed by the welding torch in the welding-based SFF process. The path generated is an outcome of both part geometry as well as process parameters of the specific SFF technique. One of the most important parameters, the torch path, $t_i \in R^3$, must allow the torch to access all points in space such that

$$X' = \sum_{i=1}^{n} \int_{0}^{L_i} \rho(t_i)\, dt_i$$

where $\rho(t_i)$ is the material feed rate over the unit length, L_i is the length of the ith layer, and n is the maximum number of layers. t_i is the torch path trajectory of the ith layer. A torch path for material deposition in SFF is driven by a geometric model of the product.

In an SFF technique such as SFF based on deposition by welding, a synthesis of the tool trajectory plays a key role. While the inability to access all regions of the geometry leads to the creation of voids in the build-up, overlaps can cause 'overdeposition' of materials. Voids and overlaps make a layer nonuniform. The uniformity of a deposited layer is of utmost importance as it determines the quality achieved in the following layers that are deposited above it.

One of the limitations of SFF based on welding is the requirement for a continuous path. Once an arc is struck, it should be sustained over the process. If the path does not connect two regions, the material deposition can be stopped when the torch is making a transition between two disconnected regions, but control of the parameters becomes more complicated. Another limitation is the requirement for maintaining the wire-feeding mechanism ahead of the torch. This requires calculation of the direction of the torch motion and, subsequently, orienting the wire-feeding mechanism. If material deposition is done only along linear segments, then the wire feeding can be stopped whenever there is a change in direction, whereas when the path is comprised of nonlinear segments the change of direction of the wire-feeding mechanism and torch motion cannot be segregated. One solution would be to break the nonlinear segments into a linear approximation, but this process would affect the quality of each layer by introducing discretization errors. In view of above two facts, a continuous path for material deposition along a contour is more generalized.

The requirements of the path-planning algorithm for a toolpath for SFF based on deposition by welding can be listed as:

- *Continuous toolpath with not more than one sweeping for any region.* The toolpath should be continuous, and there should be no overlap between the paths.
- *Minimize number of tool retractions* (Park and Choi 2000). Every tool retraction involves a change in the material feeding direction, and that change can cause irregularities in the layer.
- *Minimize number of toolpath elements* (Park and Choi 2000). With a constant feed rate, uniformity of deposition is governed by the smoothness of the path curve segments; therefore, minimizing the number of toolpath elements gives a more uniform layer.

The method to decide a suitable orientation for minimizing the number of tool retractions has been adapted from Park and Choi (2000); however, this method does not ensure that the number of elements in the path is minimum. Another method that can be looked at is the orientation of the polygon for minimum height, i.e., the minimum difference in the y-coordinates of the top and bottom vertices. A comparison of the total number of horizontal path elements for the orientation based on above methods helps in arriving at an optimal orientation.

Material Deposition and Bead Properties

The dominant parameters for SFF based on deposition by welding are welding current, welding voltage, material feeding rate, and geometry of the layer (Kmecko, Jandric, and Kovacevic 2001). Contrary to the milling process, the cross-sectional area of the bead deposited in welding is nonsquare.

The quantity of material deposited varies from the center of the bead to the edges (*Figures 2a* and *2b*). To achieve a uniform surface along the layer, two beads are deposited close enough so that the deficit of material along the edges gets compen-

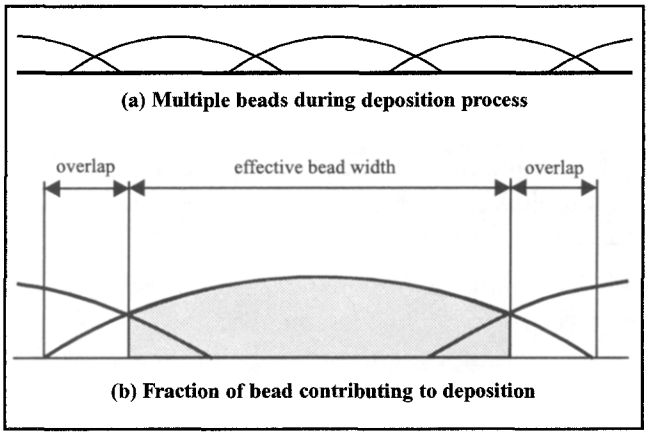

Figure 2
Fraction of Bead Width that Contributes Toward Material Deposition

sated for by an overlap between the beads (*Figure 2b*). Along the external edges of the cross-sectional area, extra material that extends beyond the effective bead gets deposited. The extra material

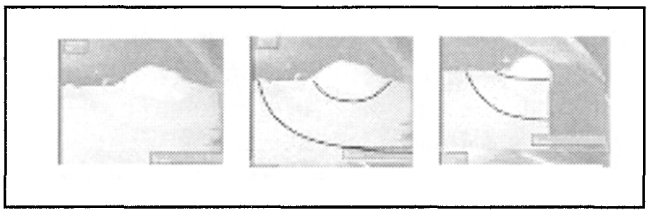

Figure 3
Photographs of Welding Bead Cross Section

is removed by the milling operation at the end of the deposition process. The movement of the material deposition head along the toolpath deposits material with a width equal to an effective bead width, as shown in *Figure 2b*.

The experimental observations (*Figure 3*) depict that the cross-sectional profile of the welding bead is similar to sinusoid. As described in *Figure 4*, the distance between two adjacent beads can be determined such that the deposition is smooth. The profile of the resultant overlap is

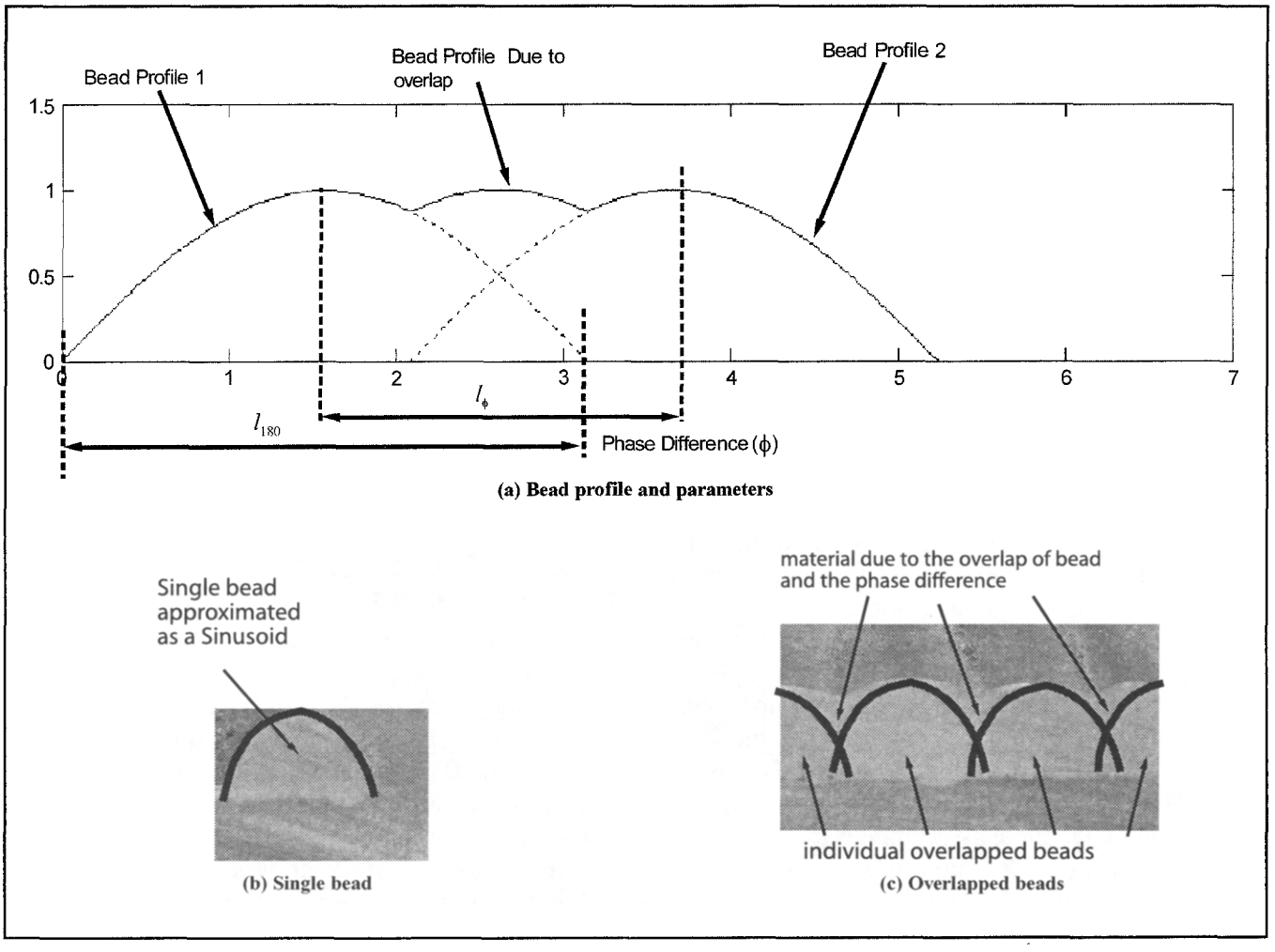

Figure 4
Approximation of Beads as Sinusoidal Curves and Overlap Profile of Beads

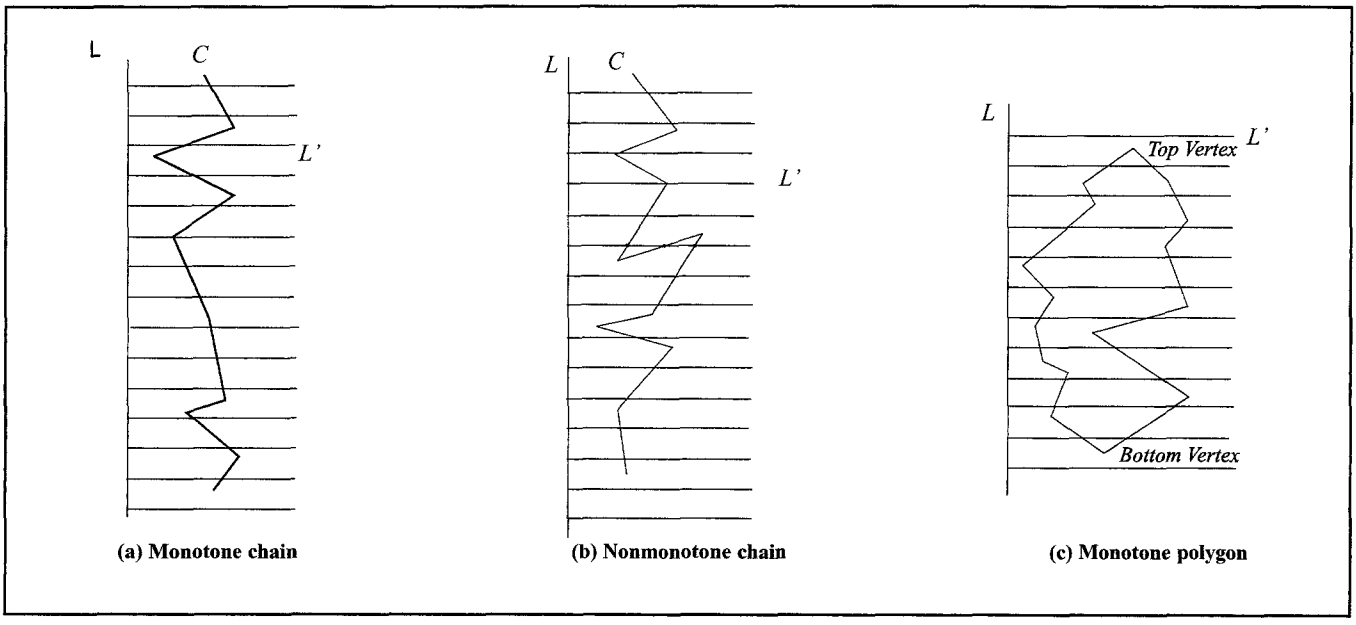

Figure 5
Monotone Chain and Nonmonotone Polygon

given by the following formula:

$$P = \sin\theta + \sin(\theta + \phi)$$

where ϕ is the equivalent phase difference maintained between two adjacent beads. The ϕ can be determined using the formula:

$$\phi = \frac{l_\phi}{l_{180}} \times 180$$

As shown in the *Figure 4a*, l_{180} is the total bead width and l_ϕ is the distance between the adjacent beads. The experimental results have shown that an equivalent phase difference of 120 degrees provides the best surface quality. The melting of the beads during the deposition process causes extra smoothness along the surfaces. *Figure 4b* shows the cross section of a single bead approximated as a sinusoid, and *Figure 4c* shows the cross section of the overlap of various beads separated by a suitable phase difference. The phase difference between the beads allows the top surface to be smooth.

Polygon Properties

Definition of Monotone Chain (Park and Choi 2000; Polygon Partitioning): A chain C is monotone with respect to line L if C has at most one intersection point with line L' perpendicular to L (*Figure 5a*).

Definition of Monotone Polygon (Polygon Partitioning; Fast Polygon Triangulation): A polygon P is considered a monotone polygon with respect to a line L if it can be split into two polygonal chains, A and B, both of which are monotone with respect to L. The two chains share the highest and lowest vertices (*Figure 5c*).

Definition of Turn Vertex (Polygon Triangulation): The vertex of a polygon is called a turn vertex when, walking along the vertices of the polygon in order, the direction of vertices changes from downward to upward or upward to downward. The turn vertex is an upturn vertex if the order of direction change is downward to upward, and the vertex is a downturn vertex if the order is upward to downward (*Figure 6*).

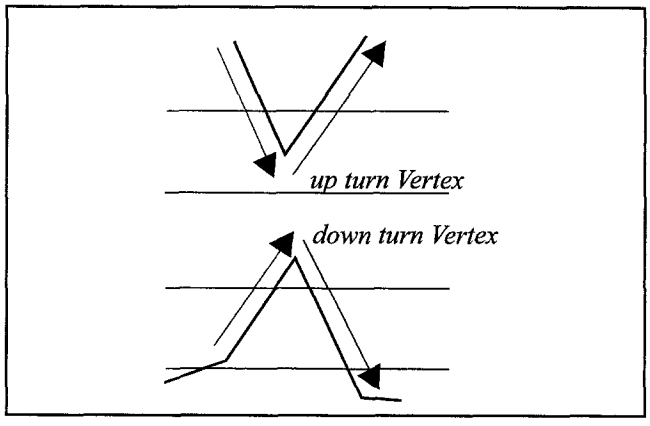

Figure 6
Upturn and Downturn Vertices

Zig-Zag Path for Monotone Polygon

The intersection of a horizontal line with the monotone polygon generates two intersection points. The y-coordinates of the two points are the same. By intersecting the monotone polygon with equidistant horizontal lines, then connecting the left and right intersection points in a consistent manner as shown in *Figure 7*, a continuous zig-zag path is obtained.

Division of Polygon to Monotone Polygons

For a polygon that is nonmonotonous, all the points along the edge of the polygon are not directly visible to each other. For such a case, the polygon can be subdivided into a set of monotone subpolygons. Paths for individual polygons can be generated and connected to obtain one continuous path for the entire cross-sectional area.

As per the definition of a monotone polygon, it can be split into two monotone chains about the highest and lowest vertices. Therefore, all the points on the monotone chain of the polygon that are at same horizontal level are directly visible to each other. By identifying all the upturn and downturn vertices in an arbitrary polygon, and projecting a line segment from the vertex to the immediate right edge of the polygon, a polygon can be divided into a set of smaller polygons for which there is the property of direct visibility; hence, the monotone polygon is satisfied (*Figure 8*).

Open and Closed Zig-Zag Paths

The starting and ending points of the zig-zag path of a monotone subpolygon are apart (*Figure 9a*); therefore, it may not be possible to connect all the paths from different subpolygons to form a continuous path. With the gap between two parallel path elements of a continuous zig-zag paths being same, it is possible to generate another zig-zag path (*Figure 9b*) (hereafter referred as a closed zig-zag path) forming a closed chain. As shown in *Figure 9c*, the end points of the closed zig-zag path for a subpolygon can be located such that it is possible to connect it to another closed

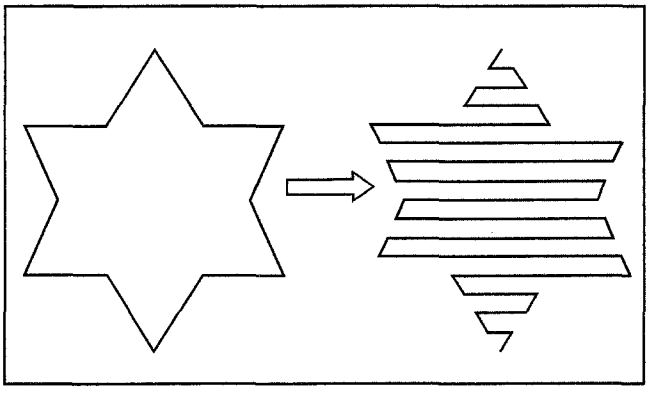

Figure 7
Continuous Zig-Zag Path Through a Monotone Polygon

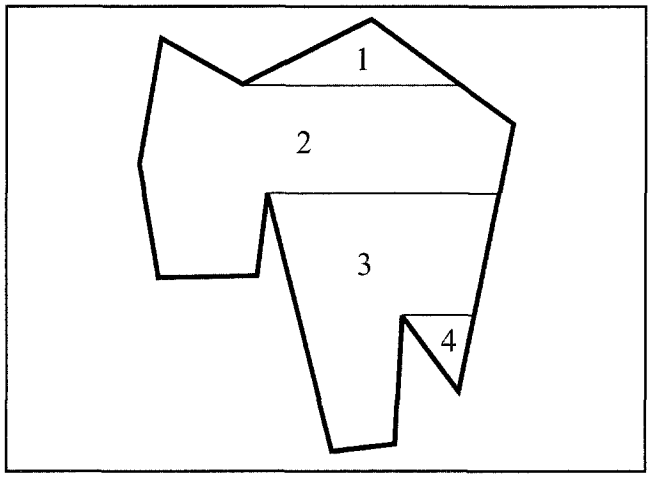

Figure 8
Polygon Divided into Set of Monotone Polygons

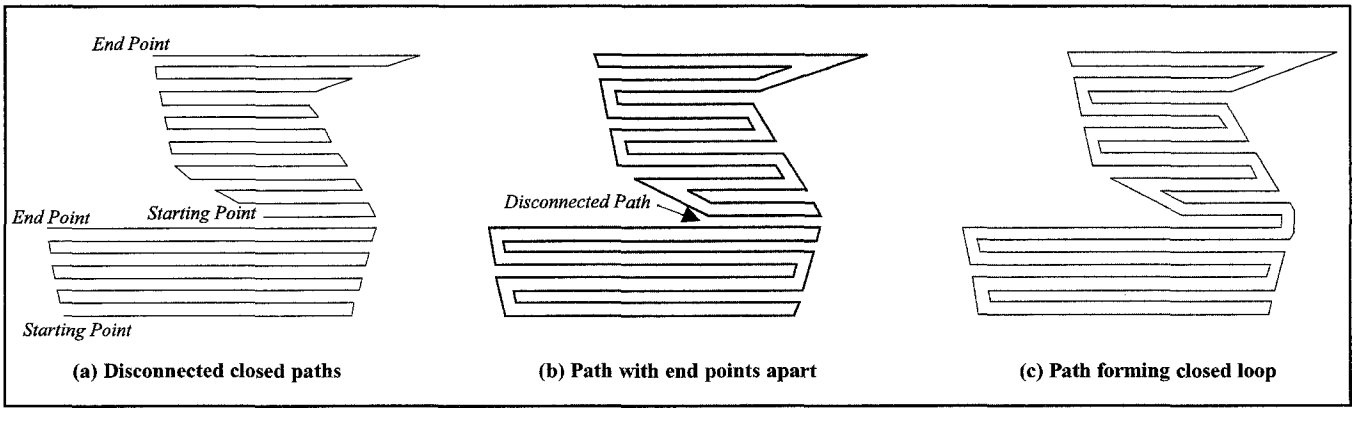

(a) Disconnected closed paths **(b) Path with end points apart** **(c) Path forming closed loop**

Figure 9
Open, Closed, and Connected Paths

zig-zag path for a subpolygon located in its proximity. This property allows connecting the paths for each of the subpolygons to form one continuous path.

Comparison of the Lengths of an Open Zig-Zag Path and a Closed Zig-Zag Path

If the bead width is relatively smaller than the lengths of the sides of a polygon, the open zig-zag path and closed zig-zag path have nearly the same length. Referring to *Figure 10*,

The length of the open zig-zag path is:

$$L_1 = 4l + 6w(\cot\alpha + \cot\beta) + w(2\operatorname{cosec}\alpha + 4\operatorname{cosec}\beta) - 2w$$

The length of the closed zig-zag path is:

$$L_2 = 4l + 6w(\cot\alpha + \cot\beta) + w(2\operatorname{cosec}\alpha + \operatorname{cosec}\beta)$$

The difference in path lengths is:

$$\Delta L = L_1 - L_2 = w(3\operatorname{cosec}\beta - 2)$$

For all practical cases, $l >> w$, ΔL is much smaller than the total path lengths, L_1 and L_2.

The zig-zag path and closed-path are formed by the repetition of the same patterns. The path shown in *Figures 10b* and *10c* replicates itself to form a zig-zag path and closed zig-zag path, respectively. The number of tool retractions and toolpath elements is approximately the same. Therefore, the mapping of the zig-zag path to a closed zig-zag path does not significantly change the quality of the material deposit. *Figure 10c* shows a zig-zag path with the number of segments equal to 7, and the number of vertices equal to 8; the same path mapped to a closed zig-zag path, as shown in *Figure 10b*, has 8 segments and 8 vertices. For most of the path, the geometry and the heat sink around the path segments is similar, therefore, the geometry of the deposition does not vary. Comparing *Figures 10b* and *10c*, it is observed that the frequency of turns along vertices 6 and 7 is higher and is enclosed by the external loop (1, 2, 3, 4); however, by using suitable control of torch speed and heat inputs along the corners, the smoothness of the surface is maintained.

Path Planning

Contour Remapping

The spacing between the paths of the subpolygons must be constant to enable a smooth deposition. To achieve consistency, the polygon should be mapped to a suitable contour (hereafter referred to as WPolygon). One of the final steps of the algorithm involves offsetting the zig-zag chains that span the polygon; therefore, the polygon is offset toward the inside to generate the WPolygon. The division of the polygon into monotone subpolygons such that the extreme edges of the adjacent subpolygons are at the same elevation allows a smooth merger of the paths for individual subpolygons during the generation of the final path. This division is accomplished in the steps for mapping the polygon to the WPolygon.

The steps for mapping the polygon to the WPolygon are described as follows:

Step 1: Offset the polygon inside by a distance equal to the bead width (*Figure 11a*).

Step 2: Identify all the turn vertices of the offset polygon.

Step 3: Classify the concave vertices of the offset polygon as upturn or downturn vertices (*Figure 11a*).

Step 4: Considering the lowest point on the offset polygon as the datum point and draw horizontal equidistant lines at an interval of two bead widths (*Figure 11b*).

Step 5: If any of the upturn (downturn) vertices lie between the two horizontal lines, extend the vertex along the y-direction to the immediate horizontal line below (above) the vertex to introduce two

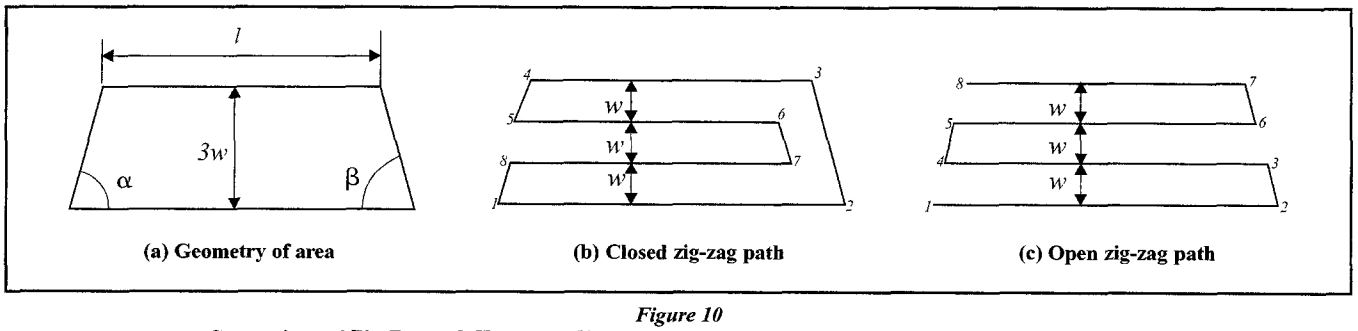

(a) Geometry of area (b) Closed zig-zag path (c) Open zig-zag path

Figure 10
Comparison of Zig-Zag and Closed Zig-Zag Path for Length, Number of Elements, and Turning Points

extra edges and sides. Introducing extra vertices provides consistent spacing between paths and thus simplifies the implementation of the algorithm. Add the vertex to the polygon such that if v_i is the initial vertex and v_a is the added vertex, then the order of vertices becomes (previous $\rightarrow v_i \rightarrow v_a \rightarrow v_i \rightarrow$ next) as shown in *Figure 12*. Classify the newly added v_a vertex to be an upturn or downturn vertex and the v_i vertex as convex. The polygon thus obtained is a WPolygon.

Partition of Contour Polygons to Subpolygons

Once the polygon is converted to the WPolygon, it should be partitioned to monotone subpolygons for path generation. The scheme for partitioning the polygon to monotone subpolygons is:

Step 1: Find the x-coordinate of the extreme right vertex of the polygon.

Step 2: Add a small positive number to the x-coordinate of the vertex. Call the new x-coordinate X_{max}.

Step 3: Extend a horizontal line from the up/down concave vertices toward the right to the point X_{max}.

Step 4: Find the point of intersection of the horizontal line with the polygon. In case there are multiple intersections, the point on the extreme left should be considered as the intersection point (*Figure 13c*).

Step 5: Join the vertex to the intersection point. This generates a monotone subpolygon. For cases in which polygons are nested (*Figure 14*), divide the polygons in order of the lowest to the topmost in hierarchy.

Notice that the mapping of the initial polygon to the WPolygon allows the end points of the polygon to be aligned with the horizontal lines mentioned in the previous section (*Figure 11b*). This alignment allows the path for each subpolygon to be compatible with respect to the paths of neighboring subpolygons.

Any polygon having internal contours can be mapped to a polygon having no contours by introducing two edges between the internal contour and the external edge of the polygon, along the lowest

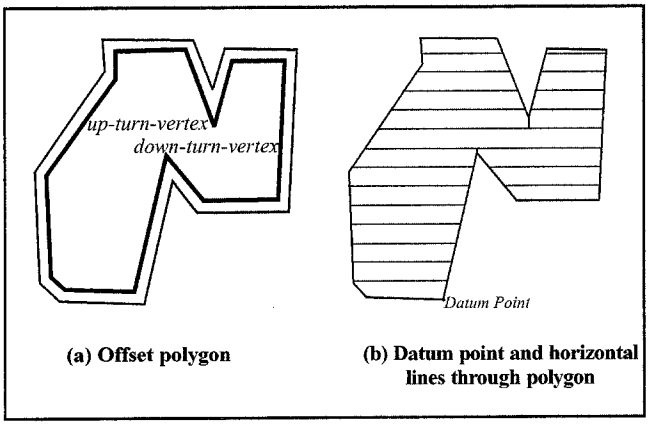

Figure 11
Offset and Vertex Classification of Polygon

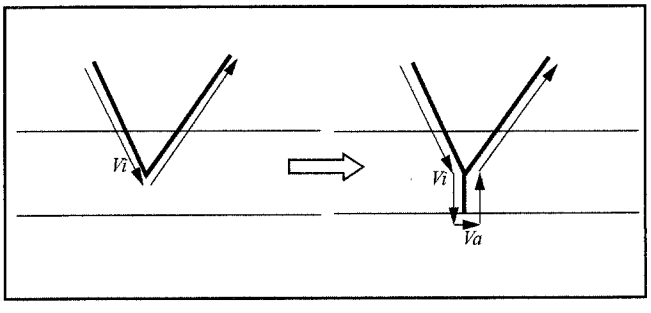

Figure 12
Mapping of Concave Points

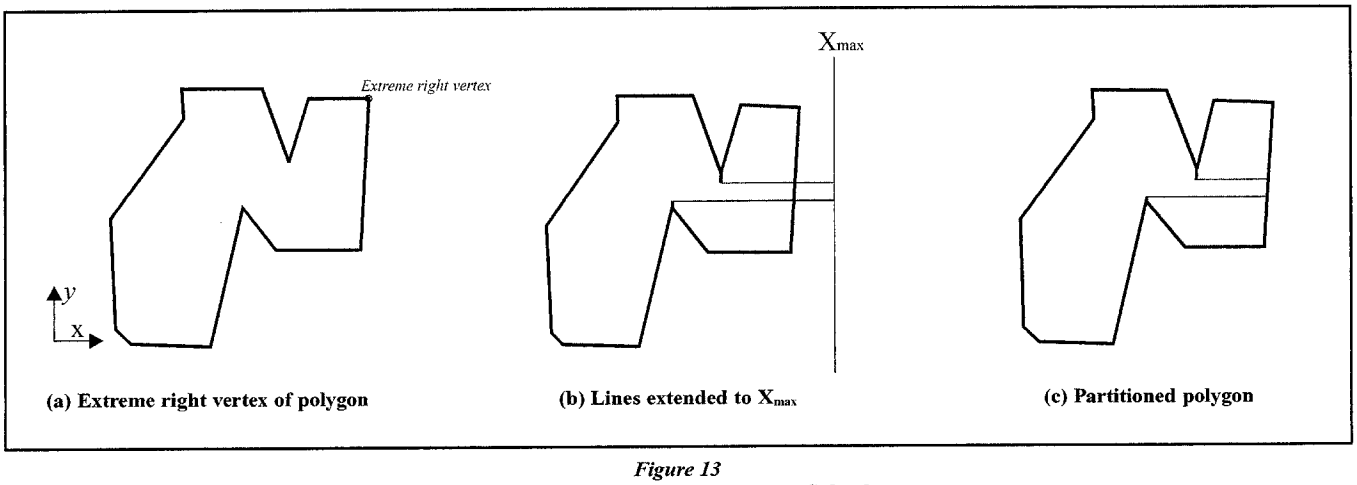

Figure 13
Mapping of Polygon to Set of Monotone Subpolygons

point of the internal contour, such that the two edges are coincident (*Figure 15b*).

The polygon thus obtained can be subdivided into monotone subpolygons (*Figure 16*).

Steps for mapping a polygon with contours to a polygon having no contours are:

Step 1: Find the lowest vertex of the internal contour.

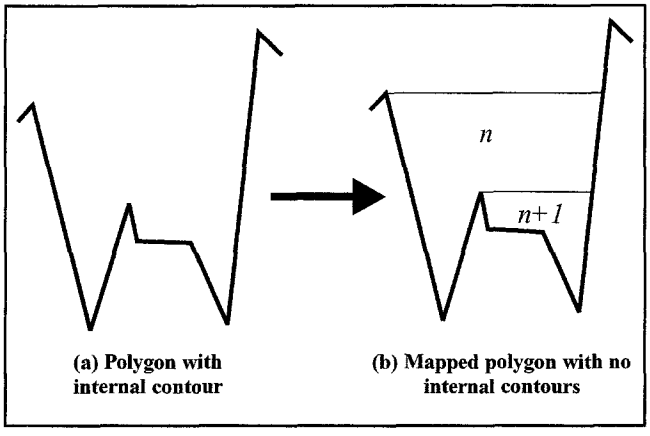

Figure 14
Nested Monotone Subpolygons

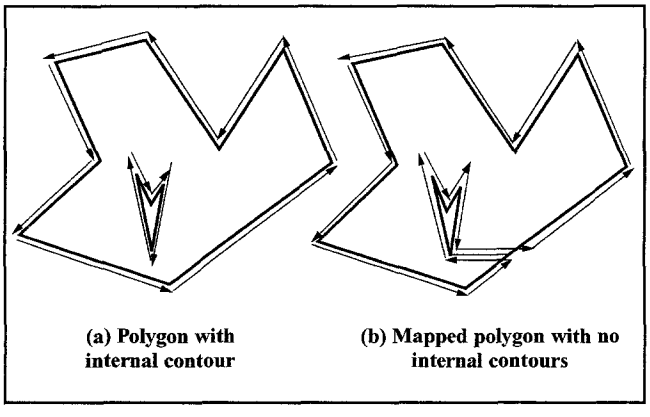

Figure 15
Mapping Polygon with Internal Contour to Polygon with No Contours

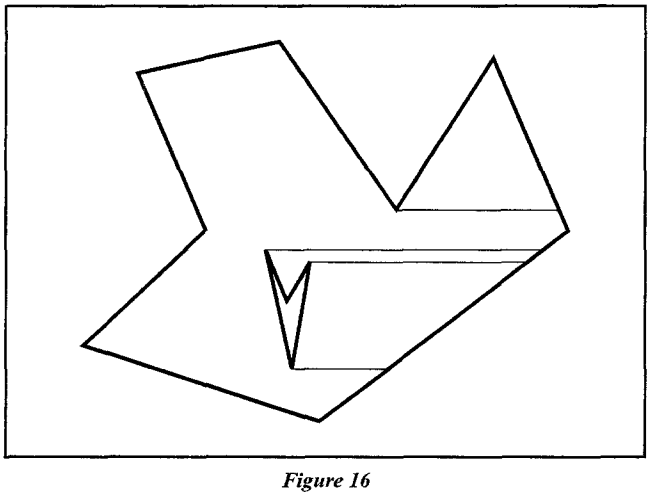

Figure 16
Polygon with Contour Mapped to Polygon with Monotone Subpolygons

Step 2: Project a horizontal line from the vertex to the right.

Step 3: Find the point of intersection of the line with external contours. In the cases where the number of intersections is more than one, consider the point of intersection having the smallest value of the x-coordinate.

Step 4 : Join the vertex and the point of intersection to get two coincident edges. The order of vertices is arranged as shown in *Figure 15b* to get the mapped polygon.

Path Generation for Monotone Subpolygons

Once the polygon is partitioned, the path can be generated by the following steps:

Step 1: With respect to the lowest point of the WPolygon as a datum point, generate a set of horizontal equispaced lines at a distance of two bead widths.

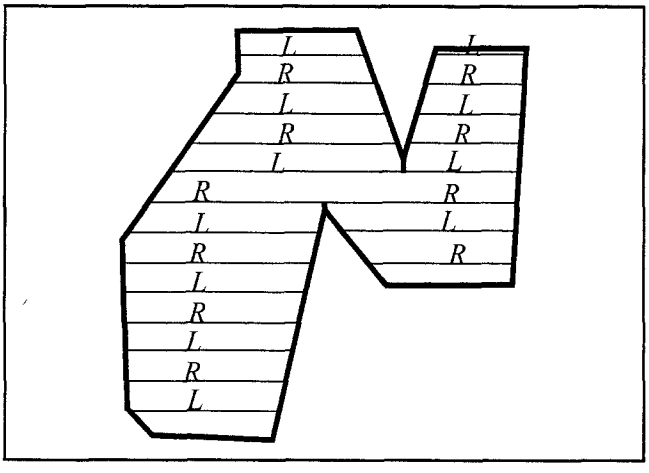

Figure 17
L-, R- Lines

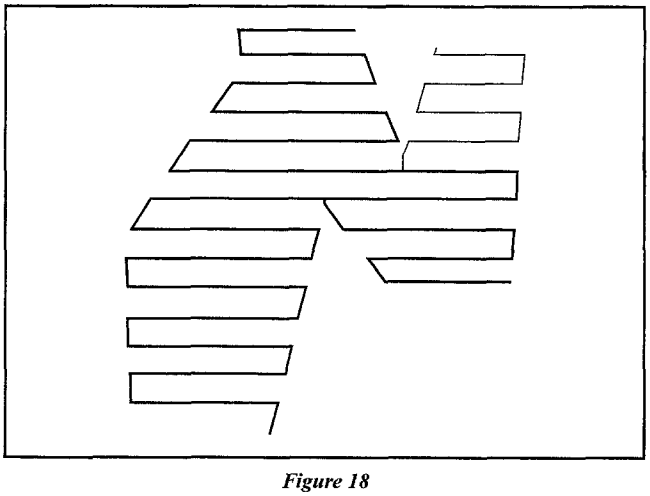

Figure 18
Zig-Zag Path for Subpolygons

Step 2: Starting with the lowest horizontal line, classify the alternate horizontal lines as R-line (right direction) and L-line (left direction) (*Figure 17*).
Step 3: Find the set of intersection points of the R-, L- lines with all the subpolygons.
Step 4: Starting from the lowest vertex in each subpolygon, form zig-zag paths for each subpolygon by connecting the intersection points along the R- and L-lines (*Figure 18*). The order of connecting the intersection points should be from right to left in the L-line and from left to right in the R-line.
Step 5: Offset the zig-zag paths on the both sides of the path by a distance equal to half the bead width (*Figure 19*).
Step 6: Offset the initial WPolygon by half the effective bead width toward the outside, and extend the end points of the offset paths to the offset of the WPolygon.
Step 7: Connect the end points of the offset paths and delete the original zig-zag path.

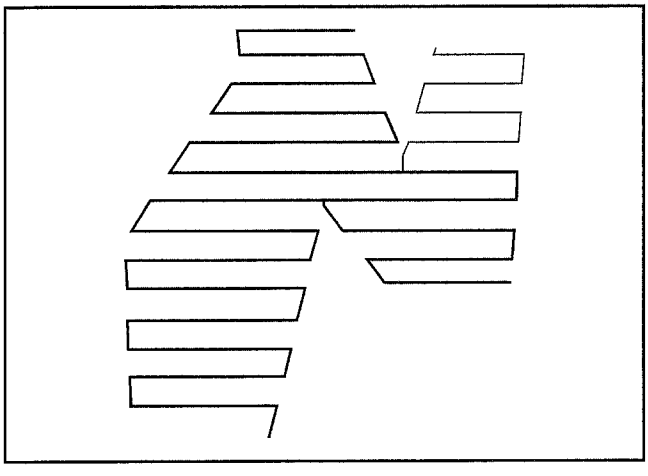

Figure 19
Offset to Zig-Zag Paths

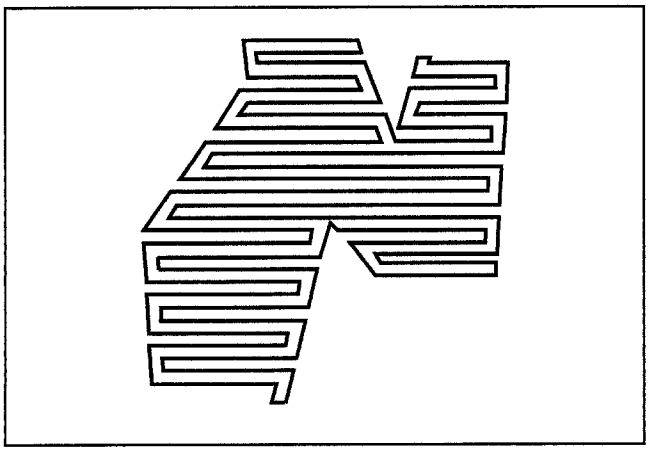

Figure 20
Final Torch Path

Generation of Final Path

Step 1: Individual subpaths of various subpolygons may be intersecting. Find the points of intersection of the subpaths.
Step 2: Trim the extension of the paths beyond the point of intersection.
Step 3: Discard any intermediate segments between two horizontal lines.
Step 4: The path generated after trimming the intersections is the final path (*Figure 20*).

Obtained Results

For the set L of all the line segments l_1, l_1 ..... l_n, that form the polygon, visiting all the segments randomly to identify all the upturn and downturn vertices of the polygon, and subsequent conversion of the polygon to a set of monotone polygons, is similar to the situation reported by Seidel (1991) for a trapezoid formation. He proves that if each permutation of l_1, l_1.....l_n, is equally likely, then trapezoid formation takes O($n$log*n) expected time, where n is the number of line segments.

The upper bound of expected time to detect the point of intersection between the offset zig-zag paths for each of the monotone polygons is O(n^2), where n is the maximum number of segments in any zig-zag path. This step can be simplified or eliminated by storing the information during polygon partition and zig-zag path generation.

The proposed method was implemented and tested with sections having linear as well as nonlinear segments. A gas tungsten arc welding torch is mounted on the end effector of a six-axis robot, and mild steel wire is fed from a spool for material deposition. The speed of the wire feeding is controlled using a mechanism based on a stepper motor. Parameters for the deposition are based on the experimental results by Jandric (2003). The torch velocity is 3.81 mm/sec., the wire feeding rate is 11.67 mm/sec., and the welding current is 90 A.

An application based on the path-planning algorithm slices the CAD model file and generates the path coordinate file. Another application is used to generate the instruction file for the robot. The robot communicates with the controller such that the wire feeding is turned off at the turning points and the rotational speed for the tool is fast enough to avoid overheating.

Figure 21 describes the path planning for a section similar to a turbine blade section profile. The cross section profile is highly nonlinear. The path generated is comprised of linear segments along the interior of the section, whereas along the external boundary the path has nonlinear segments.

Figure 22 describes the cross section, the final closed path based on the suggested scheme, and a component manufactured using the path.

Figure 21d and *Figure 22c* describe the geometry of a layer during the deposition process. *Figure 21e* describes the geometry of deposition prior to the machining. Suitable overlap between the adjacent beads allows a smooth surface profile and near-net accuracy of the fabricated part.

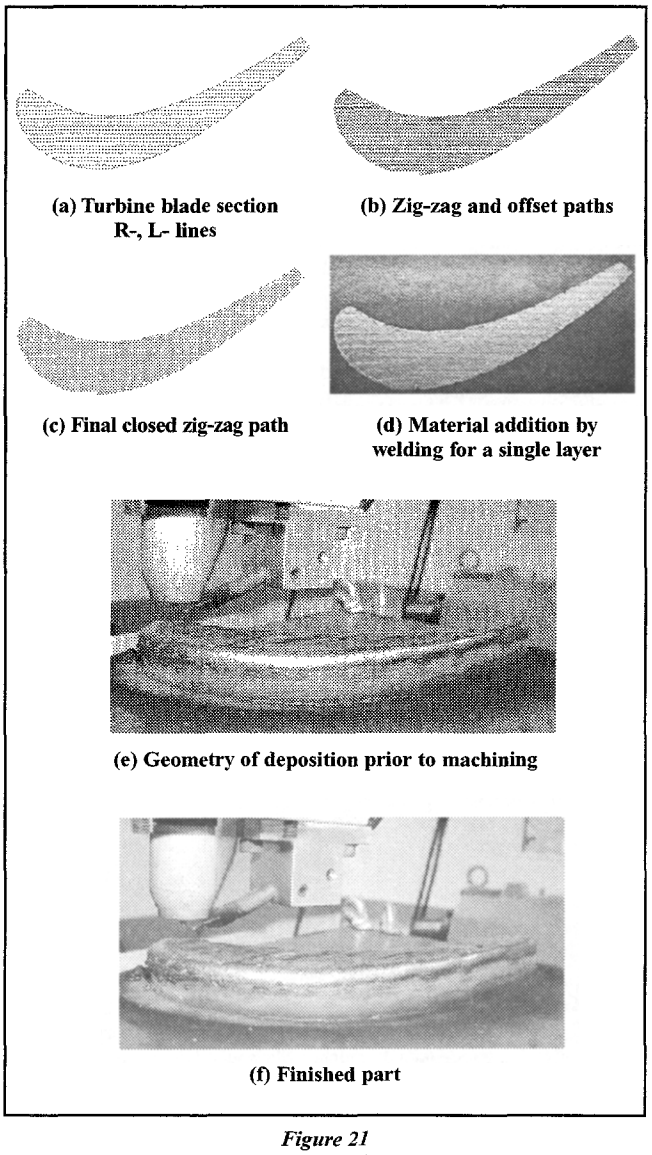

Figure 21
Torch Path for Shape of Turbine Blade

For the cross-sectional geometries that have relatively small features, such as notch-like shapes shown in the *Figure 23*, it is recommended to neglect them and represent the edge as continuous. Inclusion of the small features increases the complexity at the path planning level. The small amount of material can be removed during the machining stage.

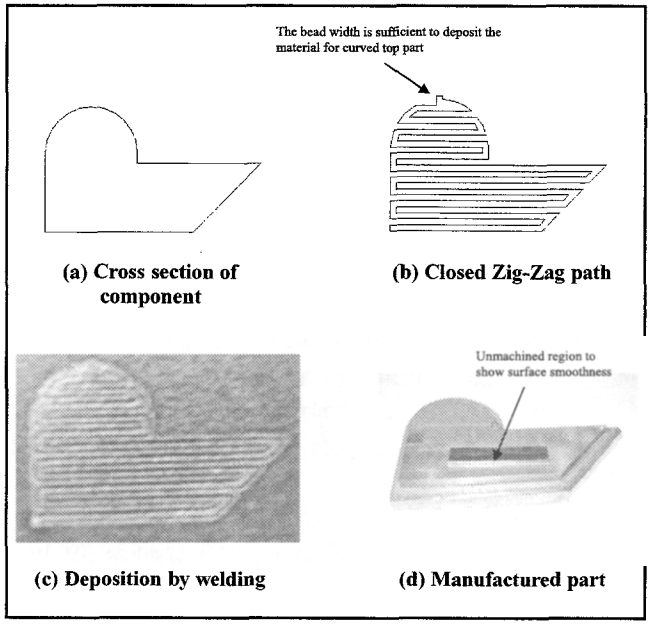

Figure 22
Manufactured Component

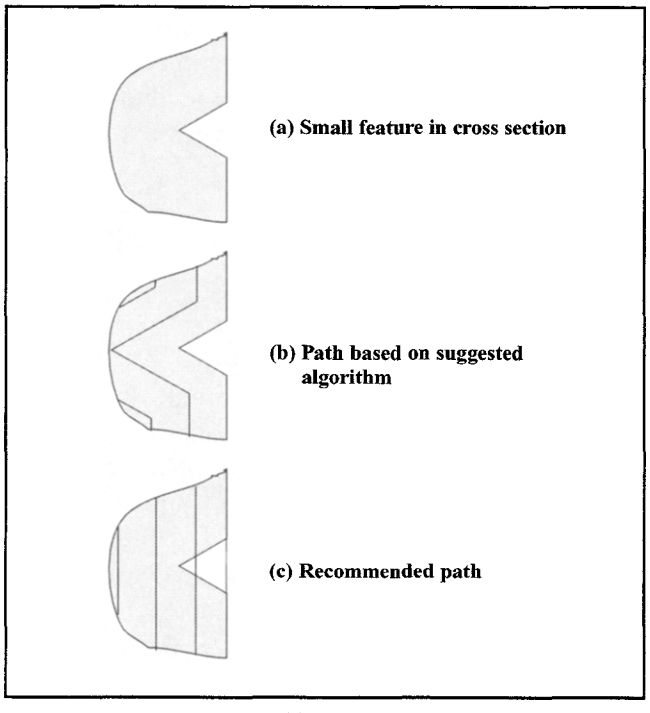

Figure 23
Approximation for Small Features in a Cross Section

Conclusions

The path planning method for SFF based on deposition by welding, as suggested in this paper, takes into account various limitations inherent in the welding process. The proposed method incorporates the requirement to achieve a continuous path. The geometric principles are used to map the initial geometry into a geometry suitable for torch path planning. The torch path for a mapped geometry, in addition to the total cross-sectional area, also deposits a small amount of extra material along the edges. The extra material is removed by the milling-after-deposition process. The obtained torch path is closed curve; therefore, the starting point of the path for a layer can be selected anywhere on the curve. This property allows connecting of the paths for subsequent layers of the model to form a continuous space curve.

The method also proposes a technique of mapping a 2-D section having internal contours to a contour suitable for application of the proposed torch path planning method. The method describes a path-generation strategy for a polygon; however, the method can be used for a nonlinear contour as well. The effectiveness of the method is supported by the experimental results.

The time complexity involved in monotone polygon generation is $O(n\log^* n)$, and for the generation of the final path is $O(m^2)$, where m is the maximum number of segments in the zig-zag path for a polygon. The total time can be reduced and certain steps can be eliminated by eliminating the redundant steps for the calculation of intersection between the zig-zag paths for each subpolygon.

For simple cases, the results were obtained using a code based on the ACIS-Kernel. The complex cases were tested using AutoCAD.

Acknowledgments

This work was financially supported by THECB (Texas Higher Education Coordinating Board) Grants 003613-0016-2001, National Science Foundation Grant DMI-0320663, and by U.S. Department of Education Grant P200A80806-98.

Authors would also like to acknowledge the help of Dr. Zoran Jandric, graduate student, and Mr. Michael Valant, research engineer, at the Research Center for Advanced Manufacturing, Southern Methodist University, for their help performing various experiments.

References

Anand, S. and Egbelu, P. (1994). "On-line robotic spray painting using machine vision." *Int'l Journal of Industrial Engg.* (v1, n1), pp87-95.

Beaman, Joseph J. (1992). "Machine issues associated with solid freeform fabrication." *Proc.* of Solid Freeform Fabrication Conf., Aug. 1992, pp309-330.

Bertoldi, M.; Yardimci, M.A.; Pistor, C.M.; and Guceri, S.I. (1998). "Domain decomposition and space filling curves in toolpath planning and generation." *Proc.* of Solid Freeform Fabrication Conf., Aug. 1998, pp267-276.

Cain, Bradley W. (1992). "Decomposition of arbitrary polygons into trapezoids." U.S. Patent 5129051, July 7, 1992.

Chen, H.; Xi, N.; and Chen, Y. (2004). "Theoretical and experimental comparison of raster and spiral tool patterns for material deposition in surface manufacturing." 2004 Japan-USA Symp. on Flexible Automation (JUSFA), July 2004.

Chen, H.; Xi, N.; Li, G.; Zhang, J.; and Saeed, A. (2004). "CAD-guided manufacturing of nanostructures using nanoparticles." IEEE/RSJ Int'l Conf. on Intelligent Robots and Systems, Sendai, Japan, Oct. 2004.

Chen, Kenwei; Crawford, Richard H.; and Beaman, Joseph J. (1996). "Parametric representation of part contours in SLS process." *Proc.* of Solid Freeform Fabrication Conf., Aug. 1996, pp597-608.

Cox, J.J.; Takezaki, Y.; Ferguson, H.R.P.; Kohkonen, K.E.; and Mulkay, E.L. (1994). "Space-filling curves in tool-path applications." *Computer-Aided Design* (v26, n3).

Crawford, Richard H.; Das, Suman; and Beaman, J.J. (1991). "Software testbed for selective laser sintering." *Proc.* of Solid Freeform Fabrication Conf., Aug. 1991, pp21-27.

Farouki, R.T.; Tarabanis, K.; Korien, J.U.; Batchelder, J.S.; and Abrams, S.B. (1994). "Offset curves in layered manufacturing." *ASME Journal of Mfg. Science and Engg.* (PED v68-2), pp557-568.

Farouki, R.T.; Koenig, T.; Tarabanis, K.A.; Korien, J.U.; and Batchelder, J.S. (1995). "Path planning with offset curve for layered fabrication processes." *Journal of Manufacturing Systems* (v14, n5), pp355-368.

Fast Polygon Triangulation based on Seidel's Algorithm. *www.cs.unc.edu/~dm/CODE/GEM*

Fossum, Gordon C. (1994). "Tesselating complex polygons in modeling coordinates." U.S. Patent 5276783, Jan. 4, 1994.

Ganesan, M. and Fadel, G. (1994). "Hollowing rapid prototyping components using offsetting techniques." 5th Int'l Rapid Prototyping Conf., Univ. of Dayton, OH, June 1994.

Griffiths, J.G. (1994). "Toolpath based on Hilbert's curve." *Computer-Aided Design* (v26, n11), pp839-844.

Held, M. (1991). *On the Computational Geometry of Pocket Machining*. Lecture Notes in Computer Science monograph (v500). Springer-Verlag.

Jacobs, P.F. (1992). *Rapid Prototyping and Manufacturing: Fundamentals of Stereolithography*. Dearborn, MI: Society of Manufacturing Engineers.

Jandric, Z. (2003). "Optimization of hybrid rapid manufacturing/repair process." PhD thesis. Dallas: Southern Methodist Univ., May 2003.

Jayanthi, Suresh; Keefe, Michael; and Gargiulo, Edward P. (1994). "Studies in stereolithography: influence of process parameters on curl distortion in photopolymer models." *Proc.* of Solid Freeform Fabrication Conf., Aug. 1994, pp250-258.

Kmecko, I.S.; Jandric, Z.; and Kovacevic, R. (2001). "Influence of geometric factor on heat transfer rate during GTAW for RP." *Proc.* of Symp. on Nontraditional Manufacturing Research and Applications, Int'l Mechanical Engg. Congress and Exposition, New York, Nov. 2001.

Li, H.; Dong, Z.; and Vicker, G.W. (1994). "Optimal toolpath pattern identification for single island sculptured part rough machining using fuzzy patterns analysis." *Computer-Aided Design* (v26, n11), pp787-795.

Park, S.C. and Choi, B.K. (2000). "Tool-path planning for direction-parallel area milling." *Computer-Aided Design* (v32) pp17-25.

Polygon Partitioning: Monotone Triangulation. *www.me.cmu.edu/faculty1/shimada/cg97/bader/*

Polygon Triangulation. *http://graphics.lcs.mit.edu/classes/6.838/F01/lectures/PolygonTriangulation/monotone.html*

Rajan, V.T.; Srinivasan, Vijay; and Tarabanis, Konstantinos A. (2001). "The optimal zigzag direction for filling a two-dimensional region." *Rapid Prototyping Journal* (v7, n5), pp231-241.

Rock, Steven J. and Wozny, Michael J. (1991). "Utilizing topological information to increase scan vector generation efficiency." *Proc.* of Solid Freeform Fabrication Conf., Aug. 1991, pp28-36.

Sarma, R. (2000). "An assessment of geometric methods in trajectory synthesis for shape-creating manufacturing operations." *Journal of Manufacturing Systems* (v19, n1), pp59-72.

Seidel, R. (1991). "A simple and fast incremental randomized algorithm for computing trapezoidal decompositions and for triangulating polygons." *Computational Geometry: Theory and Applications* (v1, n1), pp51-64.

Sheng, W.; Xi, N.; Chen, H.; Song, M.; and Chen, Y. (2003). "Surface partitioning in automated CAD-guided tool planning for additive manufacturing." Vol. 2. IEEE/RSJ Int'l Conf. on Intelligent Robots and Systems, Las Vegas, NV, Nov. 2003, pp2072-2077.

Tarabanis, Konstantinos A. (2001). "Path planning in the Proteus rapid prototyping system." *Rapid Prototyping Journal* (v7, n5), pp241-252.

Ullet, Jill S.; Chartoff, Richard P.; Lightman, Allan J.; Murphy, J.P.; and Li, Jinghong (1994). "Reducing warpage in stereolithography through novel draw styles." *Proc.* of Solid Freeform Fabrication Conf., Aug. 1994, pp242-249.

Venkataramani, Ravi; Das, Suman; and Beaman, Joseph J. (1998). "Geometry processing for SLS/HIP." *Proc.* of Solid Freeform Fabrication Conf., Aug. 1998, pp19-26.

Yang, J.; Bin, H.; Zhang, X.; and Liu, Z. (2002). "Fractal scanning path generation and control system for selective laser sintering." *Int'l Journal of Machine Tools and Manufacture* (v43), pp293-300.

Authors' Biographies

Rajeev Dwivedi received his B.Tech degree from the Indian Institute of Technology, Guwhati, India, in 1999 and MS degree in 2003 from Southern Methodist University. He is presently a PhD candidate in the Dept. of Mechanical Engineering, Southern Methodist University. He worked as a research engineer in the Computer Aided Design and Engineering Div. at the Thapar Center for Industrial Research and Development, Patiala, India. His current research includes computer-aided design, process planning, and kinematic planning for multi-degree of freedom machines for automated metal deposition and removal based on geometrical reasoning.

Dr. Radovan Kovacevic is a Herman Brown Chair Professor and director of the Research Center for Advanced Manufacturing at Southern Methodist University. His research areas of interest include advanced manufacturing processes, online monitoring and control of manufacturing and welding processes, rapid manufacturing/repair based on deposition by welding and laser cladding, and friction stir welding. Dr. Kovacevic is a Fellow of the Society of Manufacturing Engineers, the American Society of Mechanical Engineers, and the American Welding Society, as well as the recipient of the 2000 Frederick W. Taylor Research Medal presented by the Society of Manufacturing Engineers.